Steady-State and Transient Behavior of a Continuous Polyethylene Terephthalate Condensation Polymerization Process. I. Melt Transesterification Stage

A. A. KHAN and K. Y. CHOI,* *Department of Chemical and Nuclear Engineering, University of Maryland, College Park, Maryland 20742*

Synopsis

The steady-state and transient behavior of a continuous stirred-tank reactor for melt transesterification of dimethyl terephthalate with ethylene glycol in the presence of metal acetate catalyst is presented. The kinetic model includes the main transesterification reactions and side reactions leading to diethylene glycol and carboxylic acid end groups. The effect of various reactor operating parameters such as [EG]/[DMT] mole ratio and feed catalyst concentration on the product distribution under steady-state reactor operating conditions is analyzed. The dynamic process model has also been solved and the reactor transients to step changes in various reactor parameters are reported.

INTRODUCTION

Polyethylene terephthalate (PET) is one of the fastest growing thermoplastic polyesters and used widely for fibers, films, bottles, and injection-molded parts. PET is manufactured by step-growth melt polymerization process which consists of three reaction steps: (1) melt transesterification of dimethyl terephthalate (DMT) with ethylene glycol (EG), (2) prepolymerization at 250–300°C and ~ 30 mm Hg, (3) finishing polymerization at 280–300°C and < 1 mmHg. Due to the stringent industrial specifications that today's polymers must meet, the need for enhanced quality control through more effective reactor operation is now more acute than ever. For instance, in order to produce PET resins offering a combination of high strength, stiffness, dimensional stability, chemical and heat resistance, and good electrical properties, fundamental polymer properties such as molecular weight, molecular weight distribution, and unwanted side product concentrations must be controlled within limits that would not damage industrial end use requirements. The presence of diethylene glycol (DEG), even in small concentration (1–2 wt %), in final polymers causes decreased crystallinity of polymers, resulting in lowered melting point, reduced heat resistance, decreased thermal oxidative, and ultraviolet (UV) light stability.

Thus, it is important to understand the relations between reactor operating conditions and polymer properties for precise polymer quality control. The ester interchange between DMT and an excess of EG represents the first step

*To whom correspondence should be addressed.

Journal of Applied Polymer Science, Vol. 37, 707–728 (1989)

CCC 0021-8995/89/030707-22$04.00

in the manufacture of PET. In the presence of a suitable catalyst, for example, zinc acetate, a mixture of the two substances is heated at about 160–200°C until nearly the theoretical amount of methanol is formed and distilled off. The reaction product consists of *bis*-hydroxyethyl terephthalate (BHET) and minor amount of small oligomers and side products, and is converted to PET by subsequent condensation polymerization with continuous removal of the ethylene glycol formed. The efficiency of the transesterification reaction depends mainly on the reaction conditions chosen, the purity of the raw materials and the technical arrangement of the ester interchange reaction equipment. Recently, for both semibatch and continuous melt transesterification processes starting with either DMT or terephthalic acid, some modeling efforts have been reported in the literature, notably by Ravindranath and Mashelkar.[1-5] The kinetic schemes used by these workers are quite comprehensive in that every possible reaction among functional end groups present in the reaction mixture was considered. Although, there still remains the problem of estimating accurate kinetic parameters for the precise prediction of the reactor behavior, such detailed modeling provides a deeper insight into the reactor behavior. In the modeling works on continuous transesterification processes reported by those workers, the effect of various operating parameters on the steady-state reactor performance was studied. No dynamic simulation of the continuous melt transesterification reactor system has been reported. When one attempts to design the process control system for the precise control of polymer properties, an adequate dynamic process model is required. Such model should provide quantitative relations between reactor operating variables and product properties during the reactor transients. In this article, we shall analyze the steady-state and transient behavior of the melt transesterification reactor. The model used in our simulation work is in some sense a simplified version of the models considered by the authors mentioned above; however, it contains most of the essential features of the transesterification process and is more manageable for numerical computations.

MODEL DEVELOPMENT

Consider the process flow diagram for a continuous melt transesterification process shown in Figure 1. Molten DMT is fed to the ester interchange reactor which is kept under an inert atmosphere within the temperature range 180–200°C. Ethylene glycol is passed in a similar fashion to the reactor from the EG storage tank. The metal acetate catalyst (e.g., zinc acetate) is injected into the EG feed stream from the catalyst storage tank. The resultant vapors (mostly methanol, EG, and trace amounts of other volatile side products) from the combination of DMT and EG to produce *bis*-hydroxyethyl terephthalate (BHET) are rectified in the distillation column; thus, EG is refluxed back into the reactor. The more volatile components in the vapor phase are condensed in the condensor and their amounts are used to measure the extent of reaction in the liquid phase. The transesterification product is transferred to the prepolymerization reactor which is maintained between 10–30 mmHg and 280–300°C. The polymer melt is pumped to the finishing polymerization reactor, usually an extruder type or a wiped film reactor.

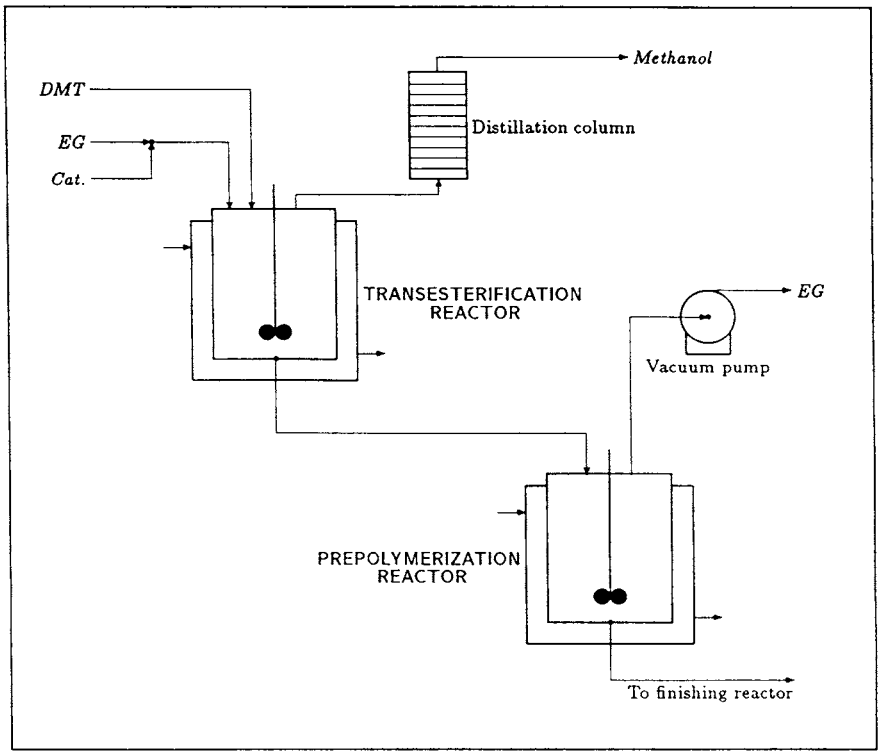

Fig. 1. Schematic diagram of continuous melt PET polymerization process.

Of the large number of possible chemical reactions postulated for the transesterification stage, we shall consider the four most important reactions. For an exhaustive evaluation of the transesterification reaction chemistry, the works of Ravindranath and Mashelkar[1] should prove to be very instructive. The motivation concerning the choice and number of reactions is to reduce the complexity posed by considering every possible reaction but also to maintain a realistic workable model which can be used for process control purposes.

Assuming that no oligomerization occurs in this stage, we can describe the main transesterification reactions as follows:

$$D + G \underset{k_1'}{\overset{k_1}{\rightleftarrows}} R_1 + M \tag{1}$$

$$R_1 + G \underset{k_2'}{\overset{k_2}{\rightleftarrows}} P_1 + M. \tag{2}$$

The chemical formulae for the symbols are shown in Table I. Since the vapor pressure of methanol is very high at the reaction temperature, it is assumed that methanol leaves the reaction mixture as soon as it is formed. When the continuous removal of liberated methanol (M) is efficiently performed, the reactions (1) and (2) can be approximated as irreversible reactions. In addition

TABLE I
Chemical Formulae for the Transesterification Model

Dimethyl terephthalate (DMT or *D*)	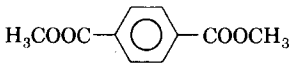
Ethylene glycol (EG or *G*)	$HOCH_2CH_2OH$
Diethylene glycol (DEG or G_D)	$HOCH_2CH_2OCH_2CH_2OH$
Methanol (M)	CH_3OH
Bis-hydroxyethyl terephthalate (BHET or P_1)	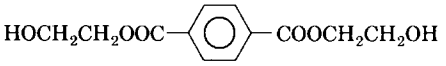
Hydroxyethyl terephthalic acid (HTPA or Q_1)	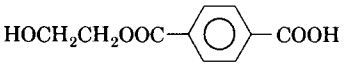
Methyl-hydroxyethyl terephthalate (MHET or R_1)	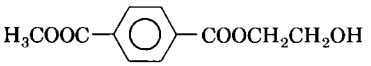
Methyl terephthalic acid (MTPA or T_1)	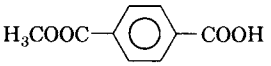

to main reactions (1) and (2), important side reactions lead to the formation of DEG, which deteriorates the properties of the final PET produced. Metal acetate catalysts, commonly used in PET production, promote side reactions which lead to the formation of DEG, acetaldehyde, acid end groups, vinyl end groups, and water. Distillation is not likely to remove DEG immediately upon formation due to its rather high boiling point, 245°C. Therefore, the side reactions considered in this work deal directly with the formation of DEG;

$$R_1 + G \xrightarrow{k_3} T_1 + G_D \tag{3}$$

$$P_1 + G \xrightarrow{k_4} Q_1 + G_D \tag{4}$$

Here, T_1 and Q_1 species contain carboxylic end groups which are formed through the reaction between EG and DEG end groups in R_1 and P_1, respectively. Acid end groups, formed in the same reaction as DEG, can participate in polymer chain growth as long as the concentration of hydroxyl end groups is high compared to acid end groups. If the acid end group formation rate is very high, then the final degree of polymerization decreases. Controlling the acid content in the polymer is very important for the thermal

stability of the polymers. According to Ravindranath and Mashelkar,[1] it is assumed that the reactivity of the methyl ester end groups on DMT and on half-esterified DMT (i.e., MHET) are the same and that the reactivity of the hydroxyl end groups on EG and on half-esterified EG are different. The reactivities of reactions (3) and (4) have also been assumed to be the same. Both oligomerization and polycondensation reactions are ignored in our model because the reaction conditions (i.e., relatively low temperature and ambient pressure) are highly unfavorable for such reactions. The temperature dependency of the rate constants is accounted for in the standard Arrhenius rate expression.

Modeling Equations

For the species defined in Table I, the material balances and energy balance have been derived and they take the following form:

Material balances:

$$V\frac{dD}{dt'} = D_0q_0 - Dq_1 - k_1VC_{cat}DG \tag{5}$$

$$V\frac{dG}{dt'} = G_0q_0 - Gq_1 - k_1VC_{cat}G - (k_2 + k_3)VC_{cat}R_1G - k_3VC_{cat}P_1G \tag{6}$$

$$V\frac{dG_D}{dt'} = G_{D_0}q_0 - G_Dq_1 + k_3VC_{cat}G(R_1 + P_1) \tag{7}$$

$$V\frac{dR_1}{dt'} = R_{1_0}q_0 + k_1VC_{cat}DG - (k_2 + k_3)VC_{cat}R_1G \tag{8}$$

$$V\frac{dP_1}{dt'} = P_{1_0}q_0 - P_1q_1 + k_2VC_{cat}R_1G - k_3VC_{cat}P_1G \tag{9}$$

$$V\frac{dQ_1}{dt'} = Q_{1_0}q_0 - Q_1q_1 + k_3VC_{cat}P_1G \tag{10}$$

$$V\frac{dT_1}{dt'} = T_{1_0}q_0 - T_1q_1 + k_3VC_{cat}R_1G \tag{11}$$

$$V\frac{dC_{cat}}{dt'} = C_{cat_0}q_0 - C_{cat}q_1 \tag{12}$$

Energy balance:

$$\begin{aligned}\rho C_pV\frac{dT}{dt'} = {} & \rho_0C_pq_0(T_0 - T_r) - \rho_1C_pq_1(T - T_r) - U_0A_c(T - T_h) \\ & - V[k_1C_{cat}DG\,\Delta H_1 + k_2C_{cat}R_1G\,\Delta H_2 \\ & \quad + k_3C_{cat}R_1G\,\Delta H_3 + k_3C_{cat}P_1G\,\Delta H_4] \\ & - V\left[\Delta H_v(T_r) + C_{p_{Mg}}(T - T_r)\right][k_1C_{cat}DG + k_2C_{cat}R_1G]\end{aligned} \tag{13}$$

TABLE II
Dimensionless Parameters

$$x_1 = \frac{D_0 - D}{D_0} \qquad x_2 = \frac{G_0 - G}{G_0} \qquad x_3 = \frac{G_D}{D_0}$$

$$x_4 = \frac{R_1}{D_0} \qquad x_5 = \frac{P_1}{D_0} \qquad x_6 = \frac{Q_1}{D_0}$$

$$x_7 = \frac{T_1}{D_0} \qquad x_8 = \frac{C_{cat_0} - C_{cat}}{C_{cat_0}} \qquad x_9 = \frac{(T - T_k)\Gamma}{T_k}$$

$$y_1 = \frac{(T_0 - T_k)\Gamma}{T_k} \qquad y_2 = \frac{(T_h - T_k)\Gamma}{T_k} \qquad y_3 = G_0\hat{V}_M$$

$$y_4 = \rho_0/\rho \qquad y_5 = \rho_1/\rho \qquad y_6 = \frac{C_{p_{M_g}}G_0}{\rho C_p}$$

$$y_7 = \frac{(T_k - T_r)\Gamma}{T_k}$$

$$z_2 = G_0/D_0 \qquad z_3 = G_{D_0}/D_0 \qquad z_4 = R_{1_0}/D_0$$
$$z_5 = P_{1_0}/D_0 \qquad z_6 = Q_{1_0}/D_0 \qquad z_7 = T_{1_0}/D_0$$

$$B_1 = \frac{\Delta H_1 G_0 \Gamma}{\rho C_p T_k} \qquad B_2 = \frac{\Delta H_2 G_0 \Gamma}{\rho C_p T_k} \qquad B_3 = \frac{\Delta H_3 G_0 \Gamma}{\rho C_p T_k}$$

$$B_4 = \frac{\Delta H_4 G_0 \Gamma}{\rho C_p T_k} \qquad B_v = \frac{\Delta H_v(T_r) G_0 \Gamma}{\rho C_p T_k} \qquad Da = k_3(T_k)\theta D_0 C_{cat_0}$$

$$r_1 = \frac{k_1(T_k)}{k_3(T_k)} \qquad r_2 = \frac{k_2(T_k)}{k_3(T_k)} \qquad t = \frac{t'}{\theta}$$

Greek letters:

$$\Gamma = \frac{E_3}{RT_k} \qquad \Gamma_1 = \frac{E_1}{E_3} \qquad \Gamma_2 = \frac{E_2}{E_3}$$

$$\theta = \frac{V}{q_0} \qquad \beta = \frac{U_0 A_c}{\rho C_p q_0}$$

Here, perfect backmixing of the reacting mixture has been assumed. Note that the catalyst material balance equation is also included in the modeling equations so that the effect of catalyst feedrate or catalyst concentration can be seen explicitly through model simulations. Since the reactor is operated at constant reactor volume, the following equation is valid for effluent stream flow rate which is subject to vary according to methanol vapor removal rate;

$$q_1 = q_0 - \hat{V}_M(k_1 V C_{cat} DG + k_2 V C_{cat} R_1 G) \tag{14}$$

where $\hat{V}_M$ denotes the molar volume of methanol.

It is convenient to put the modeling Eqs. (5)–(14) into dimensionless form. For this purpose, the dimensionless variables and parameters defined in Table II were substituted into the material and energy balances resulting in the

following dimensionless dynamic modeling equations:

$$\frac{dx_1}{dt} = -1 + q(1 - x_1)$$

$$+ z_2 Dar_1(1 - x_1)(1 - x_2)(1 - x_8)\exp\left[\frac{\Gamma_1 x_9}{1 + x_9/\Gamma}\right] \tag{15}$$

$$\frac{dx_2}{dt} = -1 + q(1 - x_2) + Dar_1(1 - x_1)(1 - x_2)(1 - x_8)\exp\left[\frac{\Gamma_1 x_9}{1 + x_9/\Gamma}\right]$$

$$+ Dar_2(1 - x_2)x_4(1 - x_8)\exp\left[\frac{\Gamma_2 x_9}{1 + x_9/\Gamma}\right]$$

$$+ Da(1 - x_2)x_4(1 - x_8)\exp\left[\frac{x_9}{1 + x_9/\Gamma}\right]$$

$$+ Da(1 - x_2)x_5(1 - x_8)\exp\left[\frac{x_9}{1 + x_9/\Gamma}\right] \tag{16}$$

$$\frac{dx_3}{dt} = z_3 - qx_3 + z_2 Da(1 - x_2)(x_4 + x_5)(1 - x_8)\exp\left[\frac{x_9}{1 + x_9/\Gamma}\right] \tag{17}$$

$$\frac{dx_4}{dt} = z_4 - qx_4 - z_2 Dar_1(1 - x_1)(1 - x_2)(1 - x_8)\exp\left[\frac{\Gamma_1 x_9}{1 + x_9/\Gamma}\right]$$

$$- z_2 Dar_2(1 - x_2)x_4(1 - x_8)\exp\left[\frac{\Gamma_2 x_9}{1 + x_9/\Gamma}\right]$$

$$- z_2 Da(1 - x_2)x_4(1 - x_8)\exp\left[\frac{x_9}{1 + x_9/\Gamma}\right] \tag{18}$$

$$\frac{dx_5}{dt} = z_5 - qx_5 + z_2 Dar_2(1 - x_2)x_4(1 - x_8)\exp\left[\frac{\Gamma_2 x_9}{1 + x_9/\Gamma}\right]$$

$$- z_2 Da(1 - x_2)x_5(1 - x_8)\exp\left[\frac{x_9}{1 + x_9/\Gamma}\right] \tag{19}$$

$$\frac{dx_6}{dt} = z_6 - qx_6 + z_2 Da(1 - x_2)x_5(1 - x_8)\exp\left[\frac{x_9}{1 + x_9/\Gamma}\right] \tag{20}$$

$$\frac{dx_7}{dt} = z_7 - qx_7 + z_2 Da(1 - x_2)x_4(1 - x_8)\exp\left[\frac{x_9}{1 + x_9/\Gamma}\right] \tag{21}$$

$$\frac{dx_8}{dt} = -1 + q(1 - x_8) \tag{22}$$

$$\begin{aligned}\frac{dx_9}{dt} = {} & y_4(y_1 + y_7) - y_5 q(x_9 + y_7) \\ & - B_1 Dar_1(1 - x_1)(1 - x_2)(1 - x_8)\exp\left[\frac{\Gamma_1 x_9}{1 + x_9/\Gamma}\right] \\ & - B_2 Dar_2(1 - x_2)x_4(1 - x_8)\exp\left[\frac{\Gamma_2 x_9}{1 + x_9/\Gamma}\right] \\ & - B_3 Da(1 - x_2)x_4(1 - x_8)\exp\left[\frac{x_9}{1 + x_9/\Gamma}\right] \\ & - B_4 Da(1 - x_2)x_5(1 - x_8)\exp\left[\frac{x_9}{1 + x_9/\Gamma}\right] - \beta(x_9 - y_2) \\ & - (B_v + y_6(x_9 + y_7)) \\ & \times \left(Dar_1(1 - x_1)(1 - x_2)(1 - x_8)\exp\left[\frac{\Gamma_1 x_9}{1 + x_9/\Gamma}\right] \right. \\ & \left. + Dar_2(1 - x_2)x_4(1 - x_8)\exp\left[\frac{\Gamma_2 x_9}{1 + x_9/\Gamma}\right]\right)\end{aligned} \tag{23}$$

where

$$\begin{aligned}q = {} & 1 - y_3 Dar_1(1 - x_1)(1 - x_2)(1 - x_8)\exp\left[\frac{\Gamma_1 x_9}{1 + x_9/\Gamma}\right] \\ & - y_3 Dar_2(1 - x_2)x_4(1 - x_8)\exp\left[\frac{\Gamma_2 x_9}{1 + x_9/\Gamma}\right]\end{aligned} \tag{24}$$

STEADY-STATE ANALYSIS

The steady-state model follows directly from the dynamic modeling equations once the left-hand side of the model equations is set to zero. The resulting nine nonlinear equations may be reduced to the following five after

some algebraic manipulations.

$$0 = -1 + q(1 - x_1) + z_2 Dar_1(1 - x_1)(1 - x_2)(1 - x_8)\exp\left[\frac{\Gamma_1 x_9}{1 + x_9/\Gamma}\right] \quad (25)$$

$$\begin{aligned} 0 = {} & -1 + q(1 - x_2) + Dar_1(1 - x_1)(1 - x_2)(1 - x_8)\exp\left[\frac{\Gamma_1 x_9}{1 + x_9/\Gamma}\right] \\ & + Dar_2(1 - x_2)x_4(1 - x_8)\exp\left[\frac{\Gamma_2 x_9}{1 + x_9/\Gamma}\right] \\ & + Da(1 - x_2)x_4(1 - x_8)\exp\left[\frac{x_9}{1 + x_9/\Gamma}\right] \\ & + Da(1 - x_2)x_5(1 - x_8)\exp\left[\frac{x_9}{1 + x_9/\Gamma}\right] \end{aligned} \quad (26)$$

$$\begin{aligned} 0 = {} & z_4 - qx_4 + z_2 Dar_1(1 - x_1)(1 - x_2)(1 - x_8)\exp\left[\frac{\Gamma_1 x_9}{1 + x_9/\Gamma}\right] \\ & - z_2 Dar_2(1 - x_2)x_4(1 - x_8)\exp\left[\frac{\Gamma_2 x_9}{1 + x_9/\Gamma}\right] \\ & - z_2 Da(1 - x_2)x_4(1 - x_8)\exp\left[\frac{x_9}{1 + x_9/\Gamma}\right] \end{aligned} \quad (27)$$

$$0 = -1 + q(1 - x_8) \quad (28)$$

$$\begin{aligned} 0 = {} & y_4(y_1 + y_7) - y_6 q(x_9 + y_7) \\ & - B_1 Dar_1(1 - x_1)(1 - x_2)(1 - x_8)\exp\left[\frac{\Gamma_1 x_9}{1 + x_9/\Gamma}\right] \\ & - B_2 Dar_2(1 - x_2)x_4(1 - x_8)\exp\left[\frac{\Gamma_2 x_9}{1 + x_9/\Gamma}\right] \\ & - B_3 Da(1 - x_2)x_4(1 - x_8)\exp\left[\frac{x_9}{1 + x_9/\Gamma}\right] \\ & - B_4 Da(1 - x_2)x_5(1 - x_8)\exp\left[\frac{x_9}{1 + x_9/\Gamma}\right] - \beta(x_9 - y_2) \\ & - (B_v + y_6(x_9 + x_7))\left(Dar_1(1 - x_1)(1 - x_2)(1 - x_8)\exp\left[\frac{\Gamma_1 x_9}{1 + x_9/\Gamma}\right] \right. \\ & \left. + Dar_2(1 - x_2)x_4(1 - x_8)\exp\left[\frac{\Gamma_2 x_9}{1 + x_9/\Gamma}\right]\right) \end{aligned} \quad (29)$$

where

$$x_3 = z_3 q^{-1} + z_2 Da(1 - x_2)(x_4 + x_5)(1 - x_8)\exp\left[\frac{x_9}{1 + x_9/\Gamma}\right] q^{-1} \quad (30)$$

$$x_5 = \frac{z_5 + z_2 Dar_2(1 - x_2)x_4(1 - x_8)\exp\left[\dfrac{\Gamma_2 x_9}{1 + x_9/\Gamma}\right]}{q + z_2 Da(1 - x_2)(1 - x_8)\exp\left[\dfrac{x_9}{1 + x_9/\Gamma}\right]} \quad (31)$$

$$x_6 = z_6 q^{-1} + z_2 Da(1 - x_2)x_5(1 - x_8)\exp\left[\frac{x_9}{1 + x_9/\Gamma}\right] q^{-1} \quad (32)$$

$$x_7 = z_7 q^{-1} + z_2 Da(1 - x_2)x_4(1 - x_8)\exp\left[\frac{x_9}{1 + x_9/\Gamma}\right] q^{-1} \quad (33)$$

The reduced steady-state model which consists of five nonlinear algebraic equations has been solved by using the mixed multivariable Newton–Raphson Regular-Falsi root finding method.[6] In order to simulate the transesterification model here as closely as possible to industrial reactors, the parameters listed in Table III have been chosen to reflect actual operating and physical conditions. Note that for process control purposes, the inlet [EG]/[DMT] mole ratio, residence time (or inlet flow rate), inlet catalyst concentration, and heating medium temperature may be used as the manipulated variables. With respect to these four variables, the base case chosen is as follows:

[EG]/[DMT] mole ratio: 1.6
Residence time: 3 h
Inlet catalyst concentration: 1.08×10^{-3} mol/L
Heating medium temperature: 180°C
Reactor volume: 1 L

Variations thereof shall be introduced to ascertain the effect of each variable on the reactor states. Initial guesses for x_1, x_2, x_4, x_8, and x_9 were input for a sequence of variations on the base case. The [EG]/[DMT] mole ratio was varied from 1.6 to 2.4, the feed catalyst/DMT mole ratio was varied from 3.0×10^{-4} to 1.0×10^{-3}, the heating medium temperature fell in the range 180–200°C. For some combinations of base case parameters, this method did not converge and for these cases the Complex Method of Box,[1,11] which is one of the constrained multivariable optimization technique was a useful alternative.

Of the nine state variables, the following variables are of particular importance: DMT conversion (x_1), ethylene glycol conversion (x_2), DEG concentration (x_3) or weight fraction, MHET (half-esterified DMT) concentration (x_4) or weight fraction, BHET concentration (x_5) or weight fraction, HTPA concentration (x_6) or weight fraction, and MTPA concentration (x_7) or weight fraction. As mentioned earlier, it is desirable to maintain minimum

TABLE III
Numerical Values of Physical Constants and Parameters

A_1	8.8513×10^9	$\frac{L^2}{mol^2\ h}$	[7]
A_2	6.0531×10^9	$\frac{L^2}{mol^2\ h}$	[7]
A_3	1.3020×10^{11}	$\frac{L^2}{mol^2\ h}$	[1]
A_c	574.0	cm^2	
C_p	0.245	$\frac{cal}{g\ K}$	[8]
$C_{p_{Mg}}$	12.60	$\frac{cal}{mol\ K}$	[8]
E_1	14340.0	$\frac{cal}{mol}$	[7]
E_2	14784.0	$\frac{cal}{mol}$	[7]
E_3	29800.0	$\frac{cal}{mol}$	[7]
ΔH_1	1400.0	$\frac{cal}{mol}$	[9]
ΔH_2	1400.0	$\frac{cal}{mol}$	[9]
ΔH_3	0.0	$\frac{cal}{mol}$	[9]
ΔH_4	0.0	$\frac{cal}{mol}$	[9]
ΔH_v	8936.0	$\frac{cal}{mol}$	[8]
T_k	450.0	K	
T_r	298.15	K	
U_0	10.0	$\frac{cal}{cm^2\ h\ K}$	[8]
$\hat{V}_M$	0.05363	$\frac{L}{mol}$	[8]
ρ	1.11	$\frac{g}{cm^3}$	
ρ_1	1.11	$\frac{g}{cm^3}$	
ρ_D	1.088	$\frac{g}{cm^3}$	[10]

DEG concentration in the product. Since BHET is the polymerizing monomer species, the transesterification reactor should be operated so as to maximize the conversion of MHET to BHET.

Figure 2 shows the effect of [EG]/[DMT] mole ratio on the steady-state reactor performance. As expected, DMT conversion increases with an increase in the mole ratio, because more EG is available to convert the DMT into either MHET or BHET. Due to the lack of experimental or plant data for continuous transesterification reactors reported in the open literature, direct

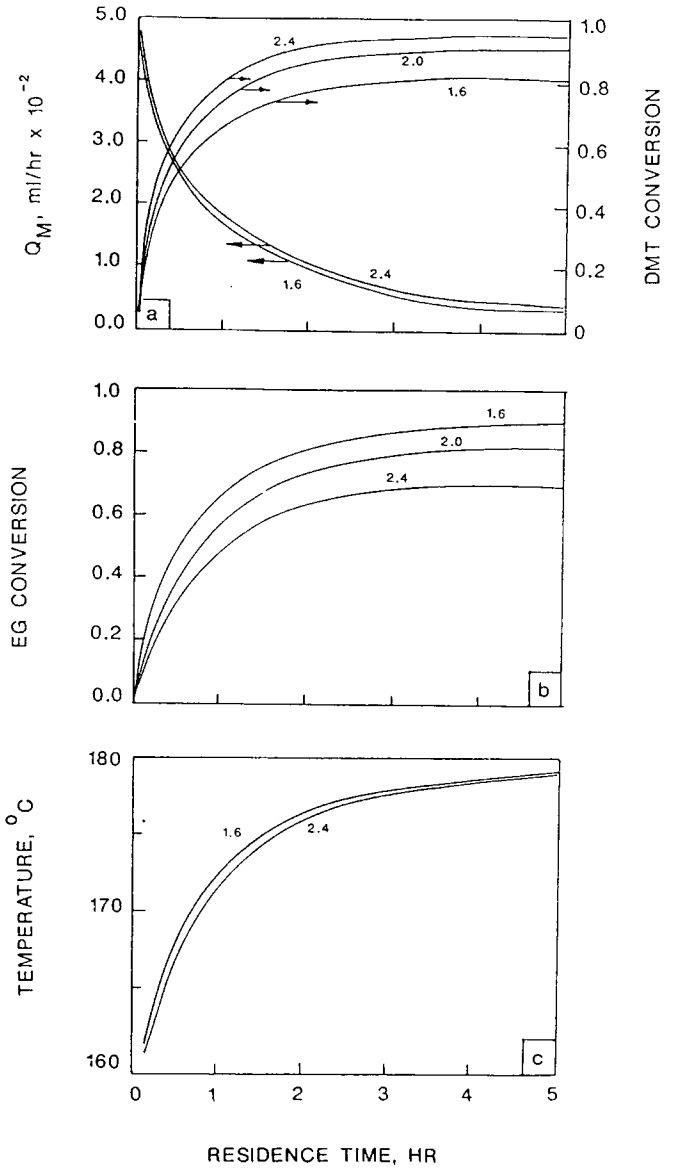

Fig. 2. Effect of feed [EG]/[DMT] mole ratio on the steady-state reactor performance.

comparison of our simulation results with experimental data was not possible. However, the observed DMT conversion versus residence time curves are qualitatively similar to that of semibatch transesterification process.[1,12] Note that [EG]/[DMT] mole ratio significantly affects the formation of DEG, in particular for large residence time. For instance, 20% increase in [EG]/[DMT] ratio almost doubles the DEG concentration for residence time of 4 h. Even for long residence times with [EG]/[DMT] = 2.4, considerable amounts of unreacted methyl ester groups are present in the reaction mixture. The concentrations of MTPA and HTPA represent the acid end groups. The sum of the concentrations of MTPA and HTPA equals the concentration of DEG

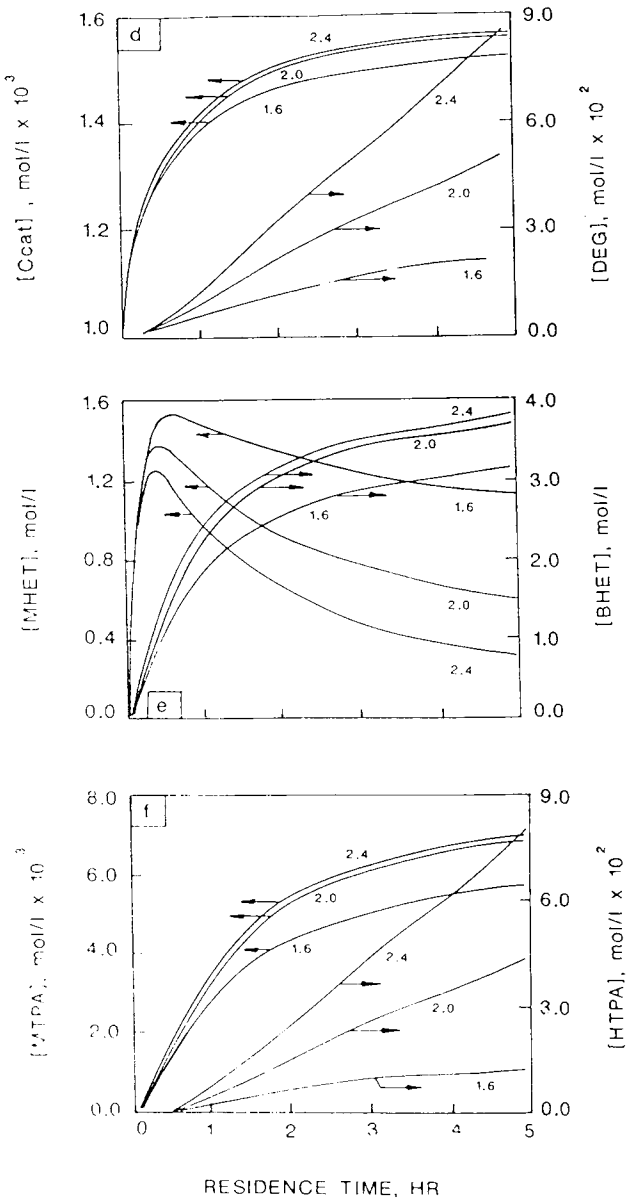

Fig. 2. (*Continued from the previous page.*)

in the reaction mixture as expected since equimolar amounts of DEG and carboxylic acid end group species are produced. More HTPA, which is significantly affected by the [EG]/[DMT] ratio, is present than MTPA because more BHET than MHET is present. The similarity of MTPA steady-state concentration profiles to those of BHET results because the same reactants, MHET and EG, cause the formation of both products.

The reactor temperature and methanol flow rate (Q_M) are largely unaffected by the choice of the [EG]/[DMT] mole ratio. However, both are appreciably changed according to the length of residence time. At short

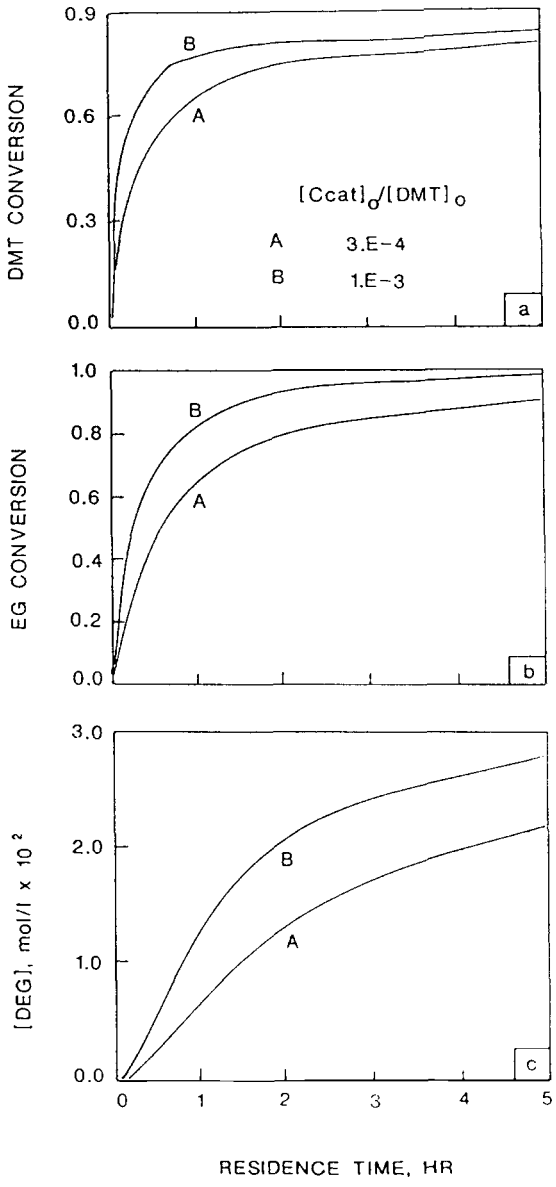

Fig. 3. Effect of feed catalyst/DMT ratio on the steady-state reactor performance.

residence times, methanol is continuously produced vigorously since the material is processed so rapidly. Thus, much heat is lost due to evaporative cooling, causing the reactor temperature to drop significantly below that of the heating medium [cf. Fig. 2(c)]. But, as residence time approaches 5 h, the four chemical reactions are allowed to proceed to near completion, thus reducing the steady-state methanol flow rate and allowing the reaction temperature to very closely approach the heating medium temperature.

The effect of catalyst concentration is illustrated in Figures 3(a)–(f). Increasing the feed catalyst concentration has the predictable effect of increas-

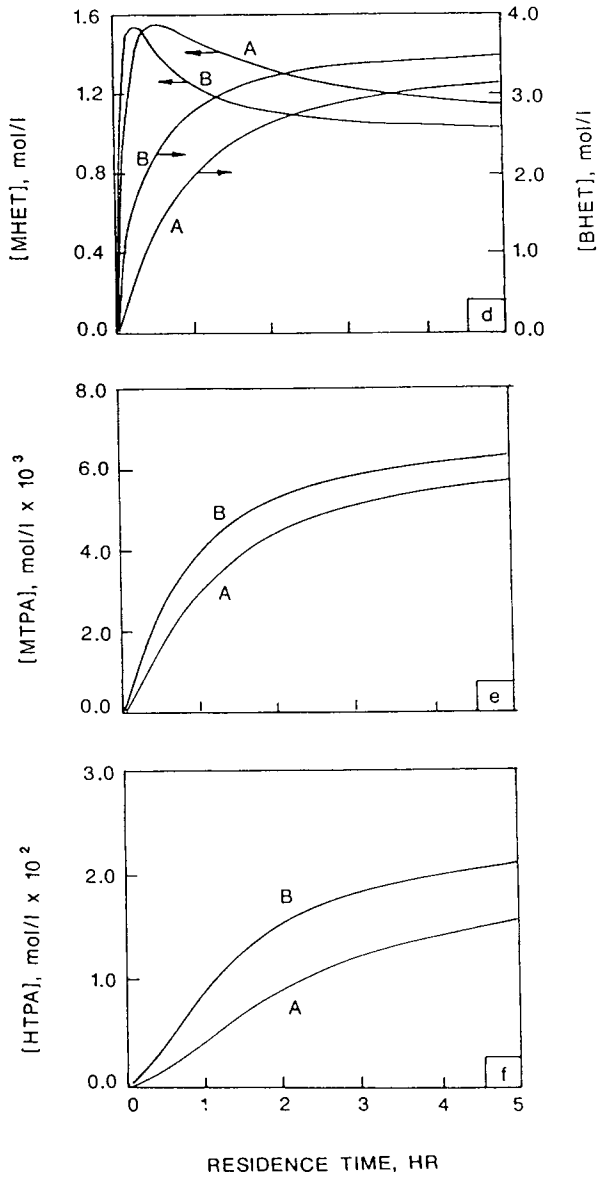

Fig. 3. *(Continued from the previous page.)*

ing both DMT and EG conversion. With increased catalyst feed concentration (i.e. $[C_{cat}]_o/[\text{DMT}]_o$ value from 3.0×10^{-4} to 1.0×10^{-3}), the concentrations of DEG and carboxylic acid end groups at long residence times increase by about 80%.

TRANSIENT BEHAVIOR

An understanding of the transient behavior of the reactor is important in designing the process control system for the precise control of polymer

properties. Since the modeling equations are highly complex, it is desirable to find reactor transients to some external disturbances through model simulations. This type of analysis will lead to the practically useful transfer function type process models. The transient response of the system is treated with respect to the step changes in the base case parameters as follows:

A. Disturbance in the [EG]/[DMT] mole ratio from 1.6 to 2.4
B. Disturbance in the feed catalyst/DMT mole ratio from 3.0×10^{-4} to 1.0×10^{-3}

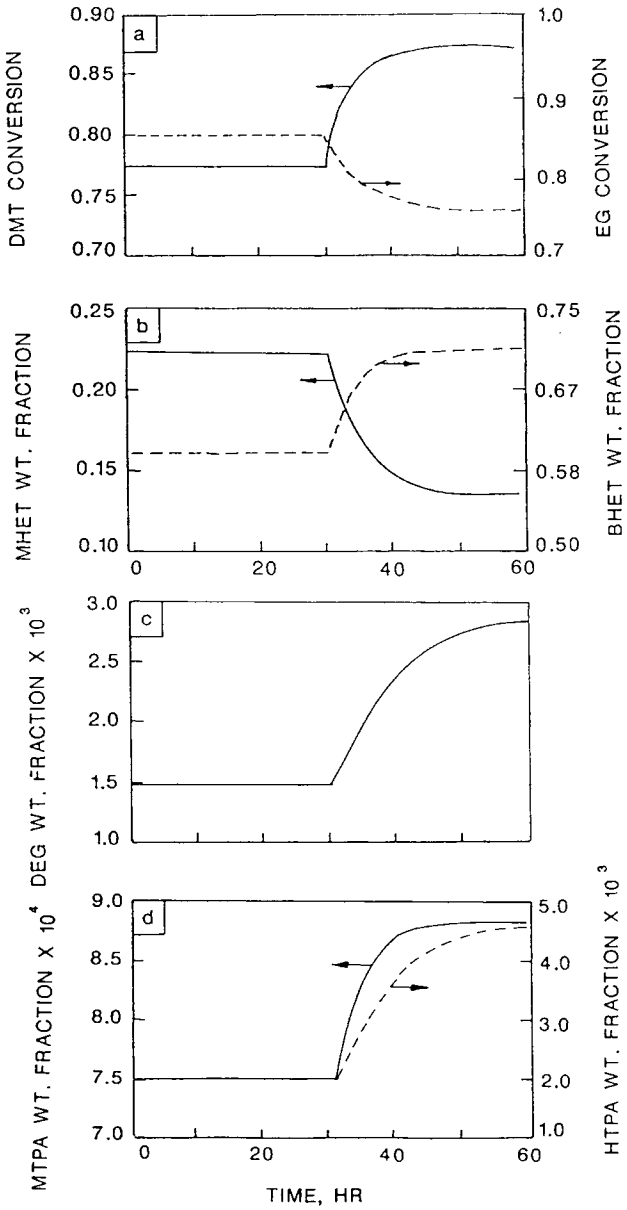

Fig. 4. Reactor transients to a step change in the feed [EG]/[DMT] mole ratio from 1.6 to 2.4.

C. Disturbance in the residence time from 3 to 2 h
D. Disturbance in heating medium temperature from 180°C to 200°C.

The dynamic modeling equations (15)–(23) were solved using the fourth-order Runge–Kutta method. The step size was 0.001 in dimensionless time, which corresponds to approximately 11 s in real time for the base case. The initial conditions for all the state variables came from the appropriate steady-state profiles computed by solving the steady-state modeling equations.

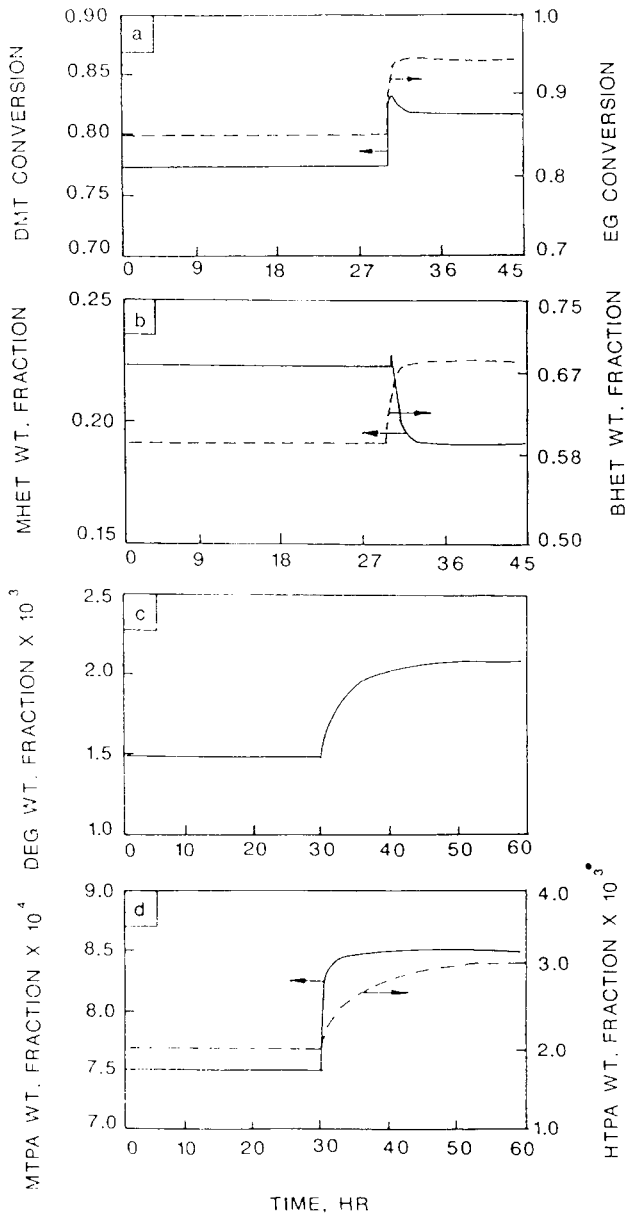

Fig. 5. Reactor transients to a step change in the feed $[C_{cat}]_o/[\mathrm{DMT}]_o$ ratio from 0.0003 to 0.001.

Figure 4 illustrates the system response to a step change in [EG]/[DMT] mole ratio in the feed stream from 1.6 to 2.4 introduced at time = 30 h. Note that the system reaches the new steady state after about four residence times (θ = 3 h). DEG concentration reaches the new steady-state value after about 6 residence times, indicating that such disturbance has a prolonged influence on some quality parameters. Although not shown, the reactor temperature decreases only by 2°C and the response was almost immediate.

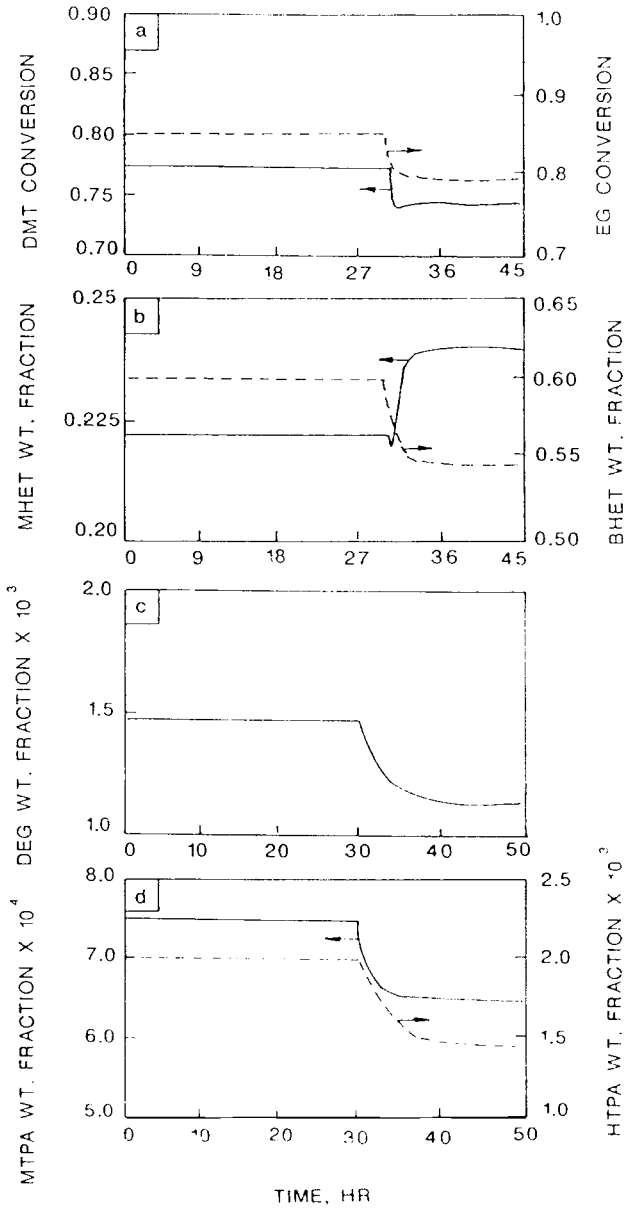

Fig. 6. Reactor transients to a step change in the reactor residence time from 3 to 2 h.

The effect of a step change in feed catalyst concentration ($[C_{cat}]_o/[DMT]_o$) from 0.0003 to 0.001 is shown in Figure 5. Note that the system variables, except DEG concentration, respond almost immediately. Small overshoots in DMT conversion and BHET concentration profiles are due to the rapid reaction at the instant when more catalyst is added to the reactor. Again, both DEG concentration and HTPA concentration take more time to reach the new steady-state concentrations.

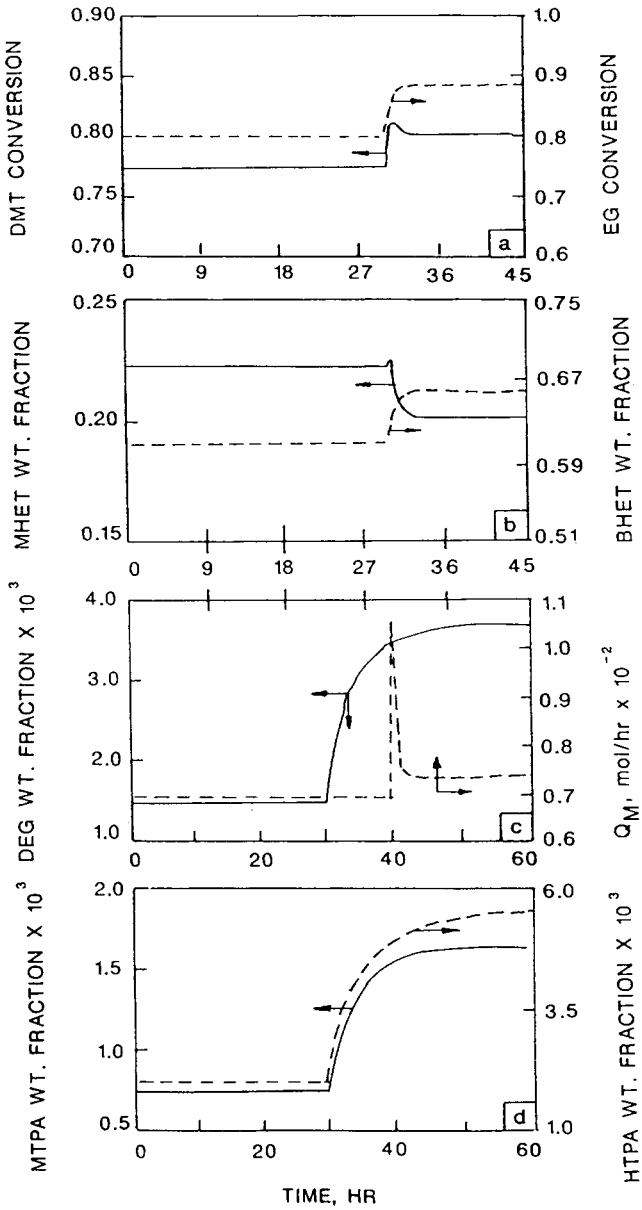

Fig. 7. Reactor transients to a step change in the heating medium temperature from 180 to 200°C.

Figure 6 illustrates the effect of step decrease in reactor residence time from 3 to 2 h by increasing the reactant feedrate. As expected, the concentrations of all the species except MHET decrease with an increase in the feedrate. Note that a 50% reduction in the reactor residence time results in a 5% decrease in DMT conversion and as much as a 25% decrease in DEG concentration.

The effect of step increase in the heating medium temperature from 180°C to 200°C is shown in Figure 7. Note that an approximate 5% increase in both DMT conversion and EG conversion is induced by the 20°C increase in the heating medium temperature. However, the DEG and carboxylic acid end group concentrations in MTPA and HTPA increase by more than 150% over the original steady-state value. The increased heating medium temperature also gives rise to the rapid increase in the methanol flow rate, which then decreases to a new steady-state value.

CONCLUDING REMARKS

In this work, we have presented the results of both steady-state and transient behavior analysis for the metal acetate-catalyzed melt transesterification in a continuous stirred tank reactor. The kinetic scheme used in our modeling includes the main transesterification reactions and side reactions to form DEG and carboxylic acid end groups. The reactor variables studied in this work (e.g., [EG]/[DMT] mole ratio, catalyst concentration, reactor temperature, and residence time) have been found to have a significant influence on the overall efficiency of the transesterification process. In particular, the DEG concentration in the reaction mixture was very sensitive to the variation in the feed [EG]/[DMT] mole ratio. Excessive evaporation of methanol has been found to occur when the feed catalyst concentration was increased. It was also observed that the response of the DEG concentration to process disturbances was much slower than that of other system variables.

This work was supported by the National Science Foundation (CBT-8504874) and in part by the Systems Research Center at the University of Maryland.

APPENDIX

Notation

A_1	frequency factor for reaction 1, L^2 mol^2/h
A_2	frequency factor for reaction 2, L^2 mol^2/h
A_3	frequency factor for reactions 3 and 4, L^2 mol^2/h
A_c	heat transfer area, cm^2
B_i	dimensionless adiabatic temperature rise for reaction i
B_v	dimensionless heat of vaporization for methanol
C_{cat}	reactor catalyst concentration, mol/L
C_{cato}	feed catalyst concentration, mol/L
C_p	heat capacity and reaction mixture, cal/g/K
C_{PMg}	molar heat capacity of methanol gas, cal/g mol/K
D	reactor DMT concentration, mol/L
D_o	feed DMT concentration, mol/L
Da	Damkohler number
E_1	activation energy for reaction 1, cal/g mol
E_2	activation energy for reaction 2, cal/g mol

E_3 activation energy for reactions 3 and 4, cal/g mol
G reactor ethylene glycol concentration, mol/L
G_o feed ethylene glycol concentration, mol/L
G_D reactor diethylene glycol concentration, mol/L
G_{Do} feed diethylene glycol concentration, mol/L
ΔH_1 heat of reaction 1 at T_r, cal/g mol
ΔH_2 heat of reaction 2 at T_r, cal/g mol
ΔH_3 heat of reaction 3 at T_r, cal/g mol
ΔH_4 heat of reaction 4 at T_r, cal/g mol
ΔH_v heat of vaporation for methanol at T_r, cal/g mol
k_1 reaction rate constant for reaction 1, L^2 mol^2/h
k_2 reaction rate constant for reaction 2, L^2 mol^2/h
k_3 reaction rate constant for reactions 3 and 4, L^2 mol^2/h
M methanol concentration, mol/L
P_1 reactor BHET concentration, mol/L
P_{1o} feed BHET concentration, mol/L
Q_1 reactor HTPA concentration, mol/L
Q_{1o} feed HTPA concentration, mol/L
q dimensionless liquid exit flow
q_o feed flow rate, L/h
q_1 exit liquid flow rate, L/h
R gas constant, cal/g mol/K
R_1 reactor MHET concentration, mol/L
R_{1o} feed MHET concentration, mol/L
r_1 ratio of reaction rate constants k_1 and k_3 at T_k
r_2 ratio of reaction rate constants k_2 and k_3 at T_k
T reactor temperature, K
T_0 feed temperature, K
T_1 reactor MTPA concentration, mol/L
T_{10} feed MTPA concentration, mol/L
T_h heating medium temperature, K
T_k non-dimensionalizing base temperature, K
T_r reference temperature, K
t' time, h
t dimensionless time
U_o overall heat transfer coefficient, $cal/cm^2/K/h$
V reactor working volume, L
$\hat{V}_M$ molar volume of methanol in desired temperature range, L/mol
W_D molecular weight of DMT, g/g mol
W_G molecular weight of EG, g/g mol
W_M molecular weight of methanol, g/g mol
x_1 DMT conversion
x_2 EG conversion
x_3 dimensionless DEG concentration
x_4 dimensionless MHET concentration
x_5 dimensionless BHET concentration
x_6 dimensionless HTPA concentration
x_7 dimensionless MTPA concentration
x_8 catalyst conversion
x_9 dimensionless reactor temperature
y_1 dimensionless feed temperature
y_2 dimensionless heating medium temperature
y_3 dimensionless methanol molar volume
y_4 ratio of inlet to reactor densities
y_5 ratio of outlet to reactor densities
y_6 dimensionless methanol heat capacity
y_7 dimensionless reference temperature
z_2 feed EG/DMT ratio
z_3 dimensionless feed DEG concentration

z_4 dimensionless feed MHET concentration
z_5 dimensionless feed BHET concentration
z_6 dimensionless feed HTPA concentration
z_7 dimensionless feed MTPA concentration

Greek Letters

β dimensionless heat transfer capability
γ feed catalyst/DMT mole ratio
ρ reaction mass density, g/L
ρ_0 feed density, g/L
ρ_1 exit flow density, g/L
Γ dimensionless activation energy
Γ_1 ratio of activation energies E_1 and E_3
Γ_2 ratio of activation energies E_2 and E_3
θ residence time, h

References

1. K. Ravindranath and R. A. Mashelkar, *J. Appl. Polym. Sci.*, **27**, 471 (1982).
2. K. Ravindranath and R. A. Mashelkar, *Polym. Eng. Sci.*, **22**(10), 610 (1982).
3. K. Ravindranath and R. A. Mashelkar, *J. Appl. Polym. Sci.*, **26**, 3179 (1981).
4. K. Ravindranath and R. A. Mashelkar, *J. Appl. Polym. Sci.*, **29**, 437 (1984).
5. A. Kumar, V. K. Sukthankar, C. P. Vaz, and S. K. Gupta, *Polym. Eng. Sci.*, **24**(3), 185 (1984).
6. A. Khan, M.S. thesis, University of Maryland, 1987.
7. K. V. Datye and H. M. Raje, *J. Appl. Polym. Sci.*, **30**, 205 (1985).
8. R. H. Perry and D. W. Green, *Chemical Engineers' Handbook*, McGraw-Hill, New York, 1984.
9. G. Challa, *Makromol. Chem.*, **38**, 105 (1960).
10. Du Pont Co. "DMT Material Safety and Data Sheet," E-77976 (1985).
11. J. L. Kuster and J. M. Mize, *Optimization Techniques with Fortran*, McGraw-Hill, New York, 1973.
12. K. Y. Choi, *Polym. Eng. Sci.*, **27**(22), 1703 (1987).

Received January 5, 1988
Accepted February 3, 1988